From L-Band Measurements to a Preliminary Channel Model for APNT

N. Schneckenburger, D. Shutin, T. Jost, M. Walter, T. Thiasiriphet, A. Filip, and M. Schnell
Deutsches Zentrum für Luft- und Raumfahrt (DLR), Germany

BIOGRAPHIES

Nicolas Schneckenburger received his Dipl.-Ing. (M.Sc.) degree in electrical engineering from the University of Ulm, Germany, in 2010. Since then he has been working as a research associate with the Institute of Communications and Navigation at the German Aerospace Center (DLR). His main focus in the last years has been ground based navigation for civil aviation and channel modeling.

Dmitriy Shutin received the Ph.D. degree in electrical engineering from Graz University of Technology (TUG), Austria, in 2006. During 2006-2009 he was an assistant professor at the Signal Processing and Speech Communication Laboratory at TUG. From 2009 to 2011 he was a research associate with the Department of Electrical Engineering at Princeton University, USA. In 2009 he was awarded the Erwin Schroedinger Research Fellowship. Since 2011 he is with the German Aerospace Center.

Thomas Jost received a Dipl.-Ing. (FH) 2001 in Electrical Engineering from University of Applied Science Wiesbaden, Germany and a Dipl.-Ing. (M.Sc) degree in 2003 in Electrical Engineering and Information Technology from Technical University of Darmstadt, Germany. In 2013, he received his PhD from University of Vigo, Spain. From 2003 to 2006 he held a research assistant position in the Signal Processing Group at TU Darmstadt. Since 2006 he is a member of the scientific staff of the German Aerospace Center.

Michael Walter received the Dipl.-Ing. (M.Sc.) degree in electrical engineering from Ulm University, Ulm, Germany, in 2008. Since 2009, he has been a member of the scientific staff of the German Aerospace Center. His research interests include wireless communications, modeling of mobile-to-mobile channels, and channel coding.

Thanawat Thiasiriphet received his M.Sc. and Ph.D. degree in electrical engineering from the University of Ulm, Germany, in 2007 and 2014 respectively. Since 2013 he has been working as a research associate with the German Aerospace Center (DLR). His current research focuses on multipath mitigation in wireless positioning systems.

Alexandra Filip received her Bachelor and Master degrees in Electrical Engineering from Jacobs University Bremen, Germany, in 2011 and 2013, respectively. In September 2013, Alexandra joined the German Aerospace Center as a research associate. Her current research focuses is on radar signal processing.

Michael Schnell received his Dipl.-Ing. (M.Sc.) and Ph.D. degree in electrical engineering in 1987 and 1997, respectively. Since 1990 he is a scientific researcher at the German Aerospace Center where he is currently group leader and project manager of the Aeronautical Communications Group. Michael Schnell is lecturer for multi-carrier communications and acts as selected advisor for the German Air Navigation Service Provider (DFS GmbH).

ABSTRACT

The paper presents results from flight trials conducted to investigate the characteristics of the L-band air to ground radio channel. Hereby, the transmitter is located on ground and the receiver in a flying aircraft.

Within the paper the setup of the measurements, including hardware setup, channel sounding method, and flight patterns, is described. The presented results include power delay profiles and multipath heatmaps for two scenarios. The results indicate that strong multipaths are present in the air to ground radio channel. It is shown, that the characteristics of the multipaths strongly depend on the distance between the receiver and transmitter.

1 INTRODUCTION

Since the early days of aviation, reliable navigation of aircraft has always been a fundamental challenge. In the future, navigation in civil aviation will increasingly rely on global navigation satellite systems (GNSS), e.g. Global Po-

sitioning System (GPS), accompanied by ground or satellite based augmentation systems (G/SBAS). Although offering a high performance, an intensified use of GNSS for aviation raises new challenges. Due to the low power levels received from in-orbit satellites, GNSS signals are susceptible to interference, both intentional, such as spoofing [1], and unintentional. Hence a navigational backup system commonly referred to as alternative positioning navigation and timing (APNT), needs to be employed. APNT offers navigation services in case of failures or unavailability of GNSS. Different ground based proposals for the APNT implementation exist for the L-Band frequency range [2, 3]. The proposals employ a network of ground-based signal transmitters.

The aircraft's position is estimated based on ranges or pseudoranges to the different ground stations. Thus, if the future APNT systems are to deliver highly accurate positioning information, it is crucial to understand the ranging characteristics of the air-to-ground (A2G) L-band wireless propagation channel. Yet this remains a challenging task, as models for the L-band A2G channel usable for testing and validating range estimators do not exist.

To gain a better understanding of the A2G channel, in 2013 DLR has conducted an extensive channel measurement campaign at the L-band. The goal is to develop a reliable L-band A2G channel model for navigation applications. A measurement bandwidth of 10 MHz is chosen enabling a thorough investigation of the channel. Different flight patterns are tested in order to allow statements of the channel characteristics under different geometrical configurations. These include flights at different altitudes and transmitter-receiver configurations, i.e. take-off and landing, as well as an enroute scenario.

The paper is organized as follows. We start by giving a description of the flight trials' setup. This includes the involved hardware, flight routes, as well as signal parameters. We proceed by giving results on the characterization of the A2G channel, such as power delay profile and multipath heatmaps. The paper is concluded by a discussion of the obtained results and an outline of the directions of future work.

2 MEASUREMENT SETUP

The goal of the flight trials is to measure the A2G channel characteristics. The setup is therefore composed of a ground station transmitter, located in a van, and an airborne receiver. Both are shown in Fig. 1. The airborne receiver records the signal, emitted from an antenna located at a known and fixed location on the ground.

2.1 Hardware setup

The transmitter hardware, located in a van, is shown in Fig. 1. A mobile transmitter is chosen to be able to travel between the aircraft at the apron and the transmit antenna's

Fig. 1. Aircraft and van carrying the receiver and transmitter hardware.

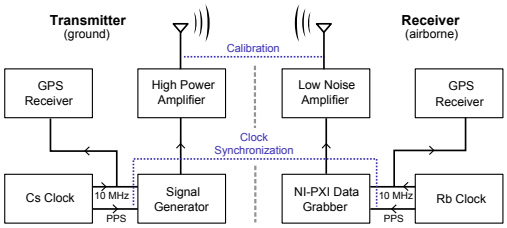

Fig. 3. Hardware setup for of receiver, located on ground, and airborne transmitter. The dotted blue lines describe the cable configuration during calibration and clock synchronization.

location. The transmit antenna is setup on top of a building 23 m above ground level (AGL) at an altitude of 652 m above mean sea level (AMSL). In Fig. 2 the area surrounding the transmit antenna, as seen from the antenna's point of view, is shown by as a 360° panorama. The transmit antenna is located in a typical airport environment: The surrounding consists of large hangar buildings, as well as smaller buildings, combined with large open spaces of either grassy or concrete surface. As transmit antenna we employ an L-band aircraft communication blade antenna (Sensor Systems S65-5366-715) with vertical polarization. Before the measurements, the antenna's position is determined by long term GPS real time kinematics (RTK) measurements with centimeter accuracy.

The transmitter hardware setup is depicted in Fig. 3 on the left side. The cesium (Cs) atomic clock acts as common time reference for the ground station's hardware. A high precision multi-frequency GNSS receiver (Septentrio PolaRx4 PRO) monitors the Cs clock by its 10 MHz signal. Thus, it continuously compares the atomic clock to the GPS time. The channel sounding sequence is generated by a signal generator, amplified using a high power amplifier (HPA), and transmitted over the antenna.

DLR's research aircraft D-CMET, a Dassault Falcon 20E, shown in Fig. 1, is used as platform for the receiver. The setup of the on-board hardware, located in three 19" racks, is depicted in Fig. 3 on the right side. A rubidium (Rb) clock acts a the common time reference for all

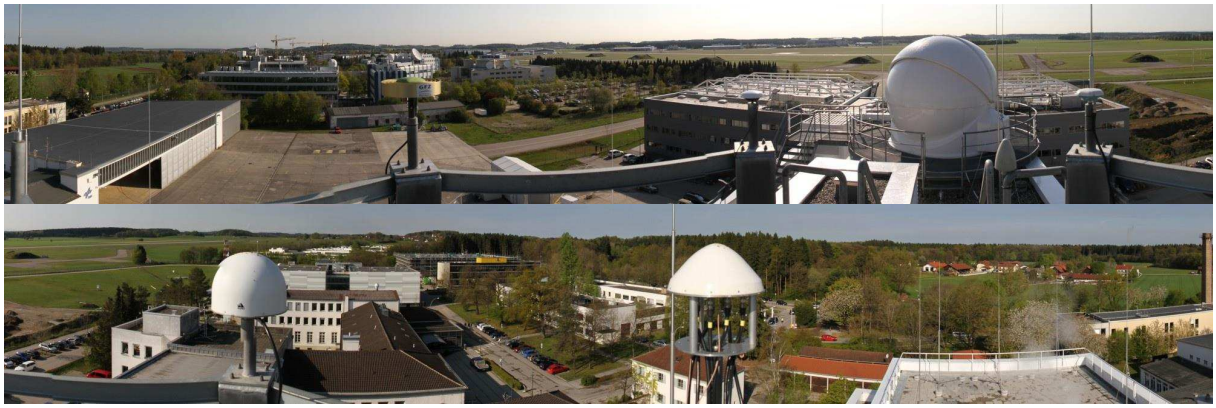

Fig. 2. Transmitter surroundings as seen from the transmit antenna's point of view.

on-board devices. The receive antenna, a commercial vertically polarized aircraft distance measurement equipment (DME) [4] antenna (Sensor Systems S65-5366-10L), is located on the bottom of the fuselage facing downwards. A low noise amplifier (LNA) amplifies the incoming signal which is then recorded by a data grabber. The data grabber based on a commercial National Instruments PXIe platform [5]. It downconverts the received signal to the baseband, samples the analog signal using a digitizer and stores it to an solid state drive (SSD) storage array. The entire PXIe system is synchronized to the Rb clock by the 10 MHz signal. The on-board multi frequency GNSS receiver (Septentrio PolaRx2e) serves two tasks: first, it acts as ground truth for the aircrafts position. Second, the GNSS receiver monitors the Rb clock and compares it to the GPS time.

The monitoring of the ground and airborne station's atomic clocks and their comparison to GPS time, allows synchronization of the receiver and transmitter. Thus, we are able to calculate the absolute propagation delay between receiver and transmitter, allowing the calculation of true ranges rather than pseudoranges. Therefore, analysis of effects leading to a bias in the propagation of the radio waves, e.g. effects caused by the troposphere, are possible.

In order to prevent an influence of the hardware setup on the measurement data, a calibration is performed prior to the channel sounding process. The calibration is performed by directly connecting the receiver and transmitter at their antenna connectors as depicted in Fig. 3. This measurement provides a zero distance calibration: Neglecting antennas delays, the receiver records the equivalent of a 0 s delay signal. That means, we are able to calibrate out all systematic errors caused by the receiver and transmitter hardware (excluding antennas).

2.2 Channel sounding sequence

The channel sounding sequence consists of a peak to average power ratio (PAPR) optimized multitone signal [6]. Its parameters are summarized in Tab. 1. The time

Parameter	Value
Carrier frequency	970 MHz
Bandwidth (Δf_{BW})	10 MHz
Transmit power (@ antenna input)	39 dBm
Used subcarriers (N_c)	5120
Symbol duration (t_{symb})	512 µs
Range resolution (d_{res})	30 m
Max. resolvable range (d_{max})	153 km
Max. resolvable freq. ($f_{\mathrm{d,max}}$)	977 kHz

Table 1. Channel sounding sequence key parameters.

period of the transmit signal is $t_{\mathrm{symb}} = 512\,\mu\mathrm{s}$, determining both the maximum resolvable Doppler frequency, $f_{\mathrm{d,max}} = (2t_{\mathrm{symb}})^{-1}$, as well as the maximum range, $d_{\mathrm{max}} = t_{\mathrm{symb}} c_{\mathrm{air}}$, which can be resolved without ambiguities, where c_{air} denotes the speed of light in air at sea level.

2.3 Flight Scenarios

Two different scenarios, enroute (ER) and approach & landing (AL), are investigated. The flight tracks and range-altitude patterns are shown in Fig. 4. Note, that for each scenario, not the complete flight's measurement data is considered. Some of the data is discarded, due to the the specific requirements, e.g. distance between receiver and transmitter or altitude, of each scenario.

- *ER:* The aircraft travels at a large range to the transmitter at normal cruising speed. During the first half of the trip the aircraft's altitude is 11 km, whereas on the way back it travels at 9 km AMSL.
- *AL:* Three missed approaches are flown at very low altitudes of 30 m to 330 m AGL. Hereby, we experience very strong banking angles of up to 45°.

The key flight parameters for each scenario are summarized in Tab. 2. The top speed observed during the measurements

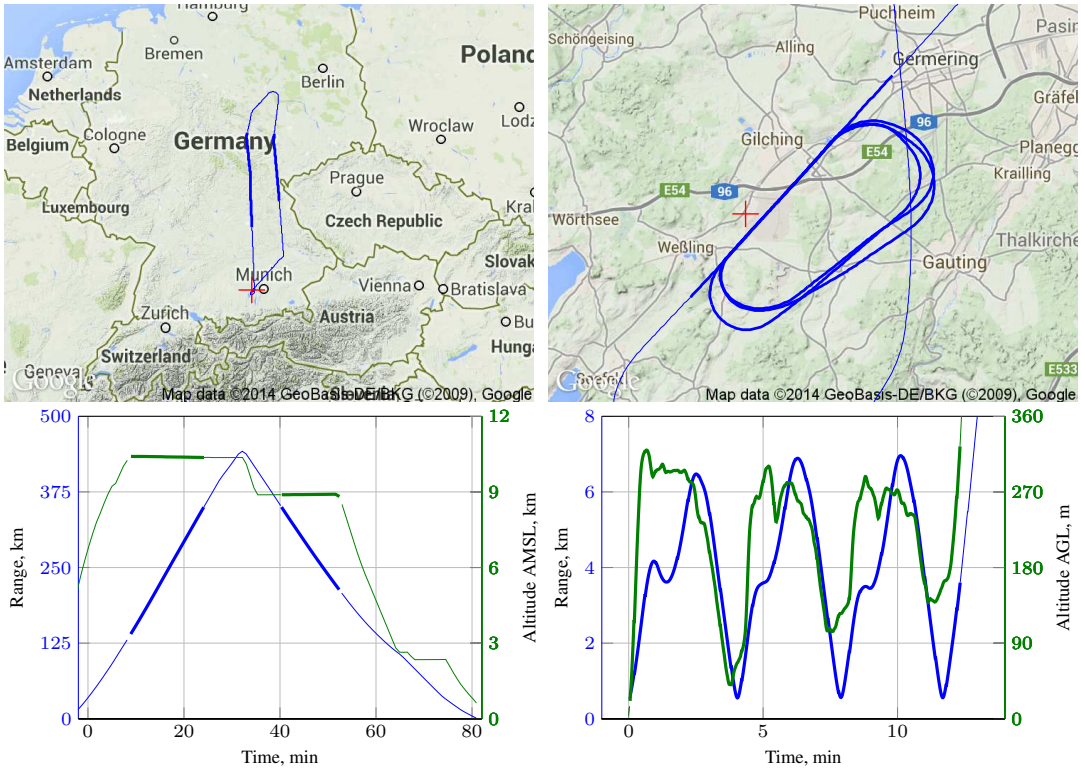

(a) Enroute (ER)

(b) Approach & landing (AL)

Fig. 4. Flight tracks and range-altitude patterns for the investigated scenarios. Locations of data points considered for a scenario are emphasized in the tracks of the entire flights. The transmit antenna's position is marked by a red cross.

Scenario	ER	AL
Duration [min]	28	14
rx-tx dist. [km]	$140 - 350$	$0.5 - 7.5$
avg.	250	4
Speed [m/s]	$192 - 235$	$67 - 105$
avg.	216	90
Altitude	$8.5 - 10.5$	$30 - 330$
avg.	9.7	213
	(km, AMSL)	(m, AGL)

Table 2. Parameters of the investigated flight scenarios.

is 235 m/s resulting in a maximum Doppler frequency of about 760 Hz.

3 CHANNEL CHARACTERISTICS

In the following section, we present results describing the multipath characteristics of the A2G channel for the two investigated scenarios.

3.1 Power Delay Profile

The power delay profile (PDP) $P_{\tau,j}(n)$ provides the average distribution of power over delay τ of the channel impulse response (CIR) for snapshot j [7]. Thus, the PDP provides information about how much power is received at a certain delay. For a better understanding of the channel's statistical properties, we estimate the probability density function (PDF) $f_{P_\tau}(p, n)$ of the PDP $P_{\tau,j}(n)$ for all j relevant for each of the scenarios. We calculate the PDF per delay bin n for $P_{\tau,j}(n)$ over the received power p. The distribution is estimated using a Kernel smoother as described in [8].

Fig. 5 shows the estimated PDF of the PDP $f_{P_\tau}(p, n)$.

Hereby, the received power is normalized to free space loss (FSL). For better readability the delay τ is scaled by the speed of light in air c_{air} and expressed as distance in meter. The plots are centered on the line-of-sight (LoS) delay. The position of the LoS's delay is estimated with a correlator rather than with the GPS based ground truth. This is done to avoid the bias introduced by the troposphere. Let us stress, that for large distances between receiver and transmitter, as for ER, up to 50 m of bias introduced by the troposphere have been observed. This bias is caused by two effects: First, the refraction of the electromagnetic waves on the different layers of the troposphere, and second, the increasing speed of light as the air thins with the increasing altitude.

From the PDF $f_{P_\tau}(p, n)$, shown in Fig. 5, the following observations are made: The ER scenario exhibits the smallest number of multiple propagation paths. Three distinct peaks can be seen at an excess delay of 360, 2500, and 3700 m. Their clean peaks indicate that each peak has a long lifetime. The long lifetime is best explained by the large distance between receiver and transmitter: the elevation change for the far away receiver is very small. Thus, the geometry under which the scattering environment close to the transmitter is observed, does not change as seen from far away. However, it is important to note, that the higher noise level may shadow weaker propagation paths. Also, due to the resolution of the 10 MHz signal, we may not be able to detect multipaths with a short excess delay compared to the LoS.

For AL scenario the PDP indicates the existence of numerous propagation paths, both distinct and diffuse. This is attributed to the small receiver-transmitter separation and the continuously changing geometry, under which the ground antenna and its scattering surrounding are seen. Compared to the ER, the power decays slower: at an excess delay of 1500 m it still significantly above the noise floor.

3.2 Multipath Heatmaps

A different way to analyze the characteristics of the channel is to observe the probability P_{ex} of experiencing a multipath component exceeding the power level P_{thres} relative to the LoS. Normalizing the power to the LoS rather than the FSL, allows to estimate the error caused by a multipath on the ranging performance using a multipath error envelope. This can be done to determine the ranging accuracy of any given APNT candidate system.

We term the resulting plots, shown in Fig. 6, as multipath heatmaps. To be able to observe the Doppler frequency of the multipath components, we combine $I = 375$ channel snapshots, allowing for a frequency resolution of $f_{\text{res}} = \frac{1}{t_{\text{symb}} * I} \approx 5$ Hz.

In Fig. 6 multipath heatmaps for the investigated scenarios are shown for two threshold levels: -10 dB and -20 dB. The white sections in the plot indicate regions, for which we are not able to make a statement about the existence of multipaths at the given threshold level P_{thres}. This is due to the width of the correlation function of the channel sounding sequence. We observe that this region is significantly larger for ER than for AL, i.e. the correlation function is wider, which can be also seen from 5(a). The increased width is mainly attributed to the existence of multipaths close to the LoS, leading to a widening of the correlation function.

For ER we conclude that all power is received on the same Doppler frequency as the LoS. The single Doppler frequency indicates that all multipath's origins lie in the direct surrounding of the transmit antenna. For the threshold $P_{\text{thres}} = -20$ dB we observe the multipath, also seen in Fig. 5(a) with a relative delay of 360 m. Due to the limited resolution, no statement about closer multipaths is possible.

For an aircraft flying in close proximity of the transmitter, as in AL, a significant contribution of power on Doppler

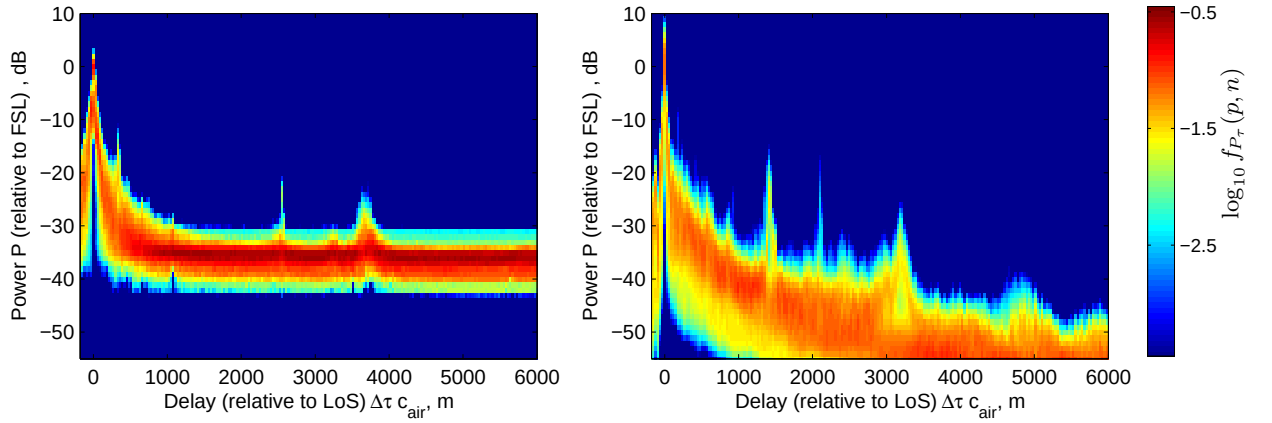

(a) Enroute (ER)

(b) Approach & landing (AL)

Fig. 5. PDF $f_{P_\tau}(p, n)$ for the investigated flight scenarios.

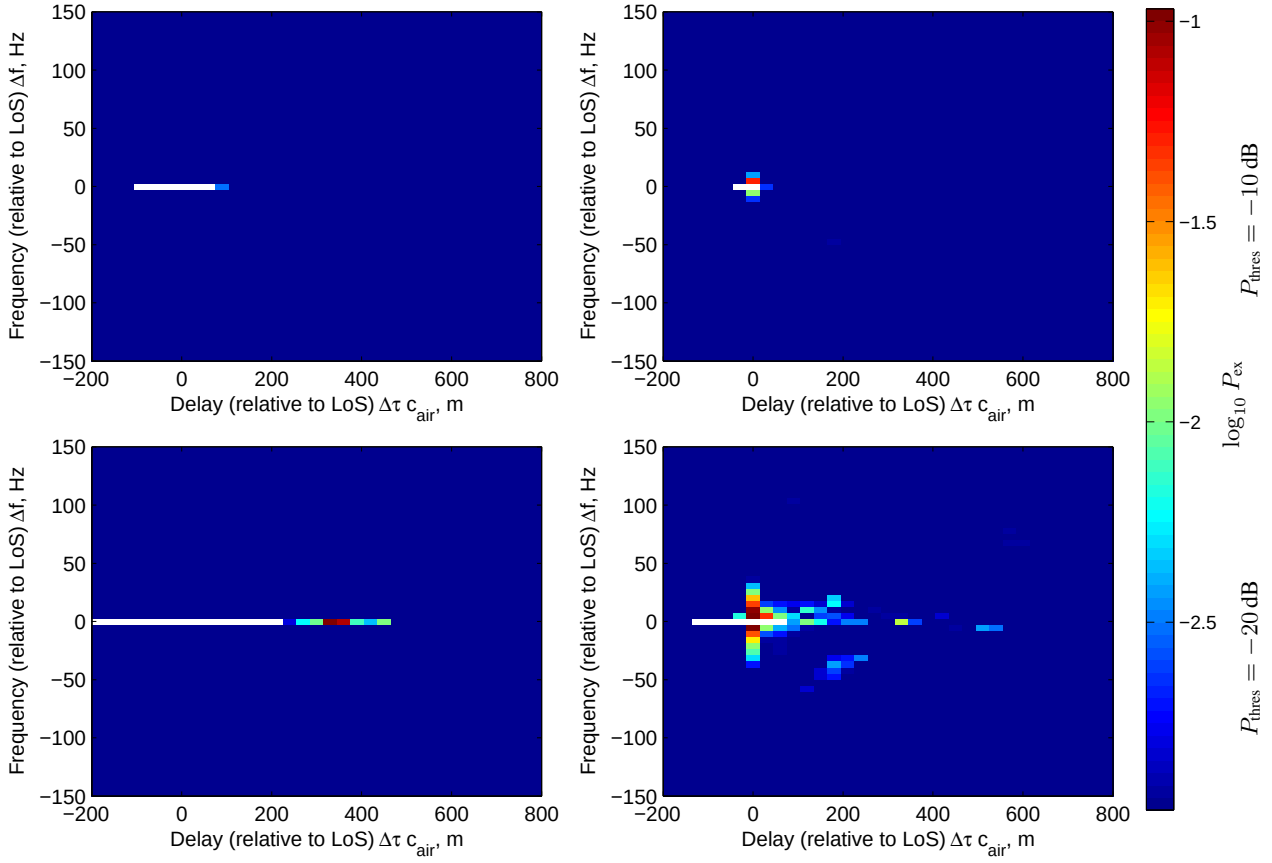

(a) Enroute (ER)

(b) Approach & landing (AL)

Fig. 6. Multipath heatmaps over delay and Doppler domain for for the investigated flight scenarios.

frequencies other than the LoS's is observed. Hence, multipaths arrive from different directions, as shown in Fig. 5(b). The result is intuitive, as the aircraft flies at very close distance to the transmitter's scattering surrounding. Thus, it sees the scatterers under different angles. The spreading of the power over the Doppler domain becomes especially apparent for the lower threshold $P_{\text{thres}} = -20\,\text{dB}$. In addition to multipaths after the LoS, we observe also a large probability for paths at the LoS delay bin. However, due to the limited resolution of the system, it is impossible to tell part of the power has to be attributed to the width of the correlation function and actually existing multipaths with a delay close to the LoS.

4 CONCLUSION AND OUTLOOK

In this paper we described a flight measurement campaign for the L-band A2G channel and presented results on the measured channel characteristics.

The A2G channel is subject to multiple propagation paths. Those multipaths have a power of up to $-6\,\text{dB}$ compared to the LoS. All observed multipaths originate from scatterers in the direct surrounding of the ground transmitter. Therefore, for larger separations between receiver and transmitter, multipaths are very distinct, have a long lifetime, and are received with a very similar Doppler frequency. In case of a smaller distance between aircraft and ground antenna multipaths become more diffuse and part of the power is also received at a different Doppler frequency than the LoS's. Using a multipath error envelope, an estimate of the ranging accuracy of any given APNT candidate system can be made using the results given above.

The future work will be focused on the development of a geometrical statistical channel model of the A2G channel. Standard methods, relying on the physical resolution of the channel sounding sequence, do not allow characterization of multipaths with a small delay and Doppler frequency relative to the LoS. Thus, in the the future, superresolution techniques will be applied in the analysis of the measurement data. The combination of superresolution and tracking allows a better characterization of the individual multipaths by parameters such as delay, Doppler frequency, amplitude and lifetime. A channel model based on this characterization will allow the generation different representations of the A2G channel, based on the measured data. The model will allow testing and validation of future APNT systems.

REFERENCES

[1] J. C. Grabowski, "Field Observations of Personal Privacy Devices," in *Proceedings of the 2012 International Technical Meeting of The Institute of Navigation*, (Newport Beach, CA), pp. 689 – 741, 2012.

[2] M. Schnell, U. Epple, D. Shutin, and N. Schneckenburger, "LDACS: Future Aeronautical Communications for Air-Traffic Management," *Communications Magazine, IEEE*, vol. 52, no. 5, pp. 104–110, 2014.

[3] S. Lo, Y. H. Chen, P. Enge, B. Peterson, and R. Erikson, "Distance Measuring Equipment Accuracy Performance Today and for Future Alternative Position Navigation and Timing (APNT)," in *Proceedings of the 26th International Technical Meeting of The Satellite Division of the Institute of Navigation (ION GNSS+ 2013)*, (Nashville, TN), pp. 711 – 721, 2013.

[4] M. Kayton and W. R. Fried, *Avionics Navigation Systems*. New York City: John Wiley & Sons, Inc., 2nd ed., 1997.

[5] N. I. P. Platform, "http://www.ni.com/pxi/."

[6] R. S. Thomä, M. Landmann, A. Richter, and U. Trautwein, *Smart Antennas - State of the Art*, pp. 241–270. EURASIP Book Series on SP&C, Hindawi Publishing Corporation, 2005.

[7] A. F. Molisch, A. Mammela, and D. P. Taylor, "Wideband wireless digital communication," 2000.

[8] B. W. Silverman, *Density Estimation for Statistic and Data Analysis*. Chapman and Hall, 1986.